Wind and Structures, Vol. 4, No. 1 (2001) 73-84
DOI: http://dx.doi.org/10.12989/was.2001.4.1.073

Characteristics of wind loads on roof cladding and fixings

J. D. Ginger†

Cyclone Structural Testing Station (CSTS), School of Engineering, James Cook University, Townsville, QLD 4811, Australia

Abstract. Analysis of pressures measured on the roof of the full-scale Texas Tech building and a 1/50 scale model of a typical house showed that the pressure fluctuations on cladding fastener and cladding-truss connection tributary areas have similar characteristics. The probability density functions of pressure fluctuations on these areas are negatively skewed from Gaussian, with pressure peak factors less than −5.5. The fluctuating pressure energy is mostly contained at full-scale frequencies of up to about 0.6 Hz. Pressure coefficients, C_p and local pressure factors, K_l given in the Australian wind load standard AS1170.2 are generally satisfactory, except for some small cladding fastener tributary areas near the edges.

Key words: wind load; cladding; cladding fastener; batten-truss connection; external pressure; internal pressure; net pressure; pressure coefficient; probability density function; Gaussian distribution; pressure spectrum.

1 Introduction

Large external suction pressures at the roof edges combined with large positive internal pressures resulting from a breach in the windward wall generates large net uplift loads that are mainly responsible for roof failure during windstorms. Wind damage investigations by Walker (1975) following cyclone Tracy which hit the city of Darwin in Australia, found that thin gauge sheet metal roof failure was initiated by fatigue cracking at the cladding fastener and the subsequent disengagement of cladding.

Presently, typical low-rise domestic house roof systems in Australia consist of battens placed at about 1.0 m intervals and attached to roof trusses installed up to 1.2 m apart as shown in Fig. 1. The roof cladding is screwed to the battens by fasteners at a spacing of 150 to 200 mm. Thin-gauge steel (~0.6 mm), "top-hat" battens shown in Fig. 1, are increasingly replacing the traditional 40 mm deep timber battens. In these systems, a cladding fastener takes wind loads acting on an area of about 0.2 m^2, whereas the batten-truss connection bears wind loads acting on a roof tributary area of 1.0 m $\times$ 1.2 m, six times the area supported by a cladding fastener. As in the case of cladding fasteners, batten-truss connections near the ridge and eaves can experience large wind loads and are also susceptible to fatigue failure at loads smaller than the ultimate limit state design load. This is a cause for concern as significant damage to large parts of a roof could arise from such failures.

Following research and extensive industry consultation, guidelines for evaluating building products for use in cyclone prone regions of Australia, TR440 (1983) were developed. According to these

† Lecturer

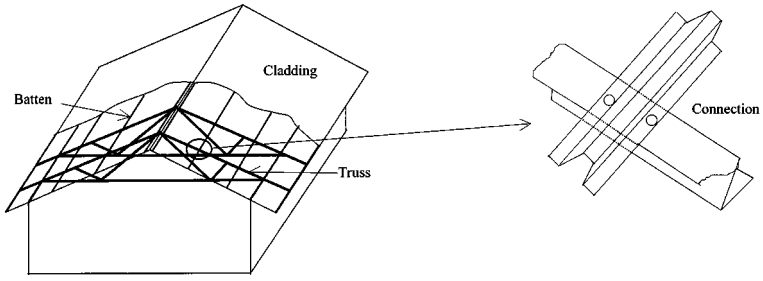

Fig. 1 Typical batten-truss layout on a domestic house roof system

guidelines which have since been included in AS1170.2 (1989), the performance of roof systems are evaluated by applying cyclic loads in the following sequence; 8000 cycles at 0-0.40 p_d, 2000 cycles at 0-0.50 p_d, 200 cycles at 0-0.65 p_d and 1 cycle at 0-1.0 p_d, where p_d is the ultimate limit state net design pressure. The loading criterion is applicable for testing cladding, its fixings and their supporting structural elements which also includes the battens. The net pressure is calculated by combining external and internal pressures acting on the tributary area of interest. Generally, internal pressure generated due to a dominant opening is applied in cyclone regions. AS1170.2 prescribes a local pressure factor K_l of 1.5 and 2.0 to be applied with negative external pressures on areas of extent less than $1.0a^2$ and $0.25a^2$ within a distance of $1.0a$ and $0.5a$ respectively from roof edges, where 'a' is taken to be the minimum of $0.2\times b$(breadth) or $0.2\times d$(depth) or h(height) of the structure.

Despite the acceptance of TR440 as the standard test requirement for evaluating building components used in most cyclone prone regions of Australia, it is criticised on a number of aspects including the load ranges and the number and sequence of loading cycles. Jancauskas *et al.* (1989) combined wind tunnel data with parameters from an artificial "design cyclone" closely matching cyclone Tracy, and generated more realistic loading cycles based on the rainflow count method. Following this and other similar studies a revamped loading regime has been proposed for inclusion in industry standards.

Reardon *et al.* (1999) carried out a structural assessment of the housing stock in Exmouth, a small township in Western Australia, after it was hit by cyclone Vance. Exmouth is located within the most cyclone prone region in Australia, region *D* as per AS1170.2, which stipulates an ultimate limit state design wind speed of 85 m/s. Based on wind speed measurements at the nearby Bureau of Meteorology station and damage to simple structures such as sign-posts etc., the peak gust wind speeds in Exmouth during Vance were estimated at between 55 and 70 m/s in the sheltered and exposed parts of town respectively. Fatigue failure of cladding fasteners commonly found in Darwin after cyclone Tracy, was not evident in Exmouth after cyclone Vance. This was partly attributed to improved design of new roofs to satisfy TR440 requirements, and the fact that the older roofs had been upgraded by installing cyclone washers and roofing screws to attach the cladding to battens. However, a number of older roof failures at the batten-rafter connection as shown in Fig. 2, were found, where generally no attempt had been made to improve the batten to truss (or rafter) connection. In most cases only two (and in some cases one) 90 mm nails were used through 50 mm battens.

The validity of applying loads specified in TR440 and AS1170.2 on tributary areas supported by batten-truss connections, albeit usually derived with a smaller pressure factor K_l than that applied to a cladding fastener, is frequently queried by roofing system designers. This paper deals with the pressure characteristics on panels representative of cladding fastener and batten-truss connection tributaries, obtained from the full-scale Texas Tech building and a wind tunnel study on a typical low-rise

Fig. 2 Failure of roof at the batten-truss connection during cyclone Vance in Exmouth WA.

house roofs. The application of K_l pressure factors derived from AS1170.2 on cladding fastener and batten-truss connection tributaries is also investigated in this study.

2. Theory

The pressure fluctuations on the roof (described by the pressure coefficient referenced to the mean dynamic pressure at the roof height, $C_p = p/(1/2)\rho\overline{U}^2$) are analysed to give the mean value over time $C_{\bar{p}}$, the standard deviation $C_{\sigma p}$, the maximum $C_{\hat{p}}$, and the minimum $C_{\check{p}}$. A normalised pressure $g_p = (C_p - C_{\bar{p}})/C_{\sigma p}$ is defined such that maximum and minimum, pressure peak factors are $g_{\hat{p}} = (C_{\hat{p}} - C_{\bar{p}})/C_{\sigma p}$ and $g_{\check{p}} = (C_{\check{p}} - C_{\bar{p}})/C_{\sigma p}$. Model and full-scale studies by Ginger and Letchford (1993) and Xu (1993) have shown that the probability density function $p_f(g_p)$ of point pressure fluctuations in separated flow regions is not of the Gaussian form of Eq. (1), but negatively skewed.

$$p_f(g_p) = (1/\sqrt{2\pi})\exp^{-(g_p^2/2)} \tag{1}$$

Ginger and Letchford (1999) showed that the windward wall pressure spectrum closely follows the energy distribution in the approach wind velocity spectrum. However a greater proportion of the fluctuating pressure energy on the roof is contained at higher frequencies compared to the approach velocity fluctuations. The net pressure spectrum on the building envelope is influenced by the internal pressure characteristics. The internal pressure fluctuations are small in a nominally sealed house, but follows the pressure fluctuations at the opening in a house containing a dominant opening.

3 Experimental set-up

The 13.7 (b) × 9.1 (d) × 4.0 (h) m full-scale Texas Tech, Wind Engineering Research Field Laboratory test building shown in Fig. 3, has an estimated nominal internal volume of 470 m^3. The building is located in terrain category 2 as per AS1170.2, and the surrounding topography is flat. External and

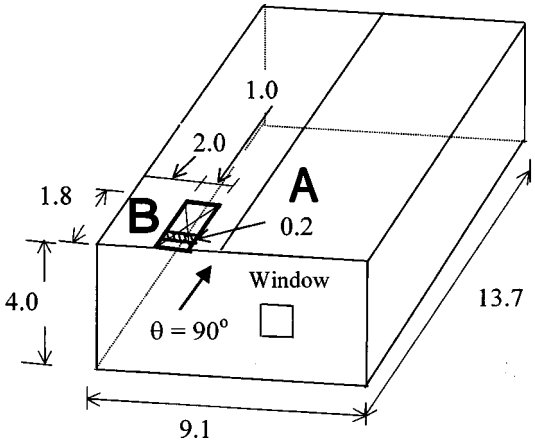

Fig. 3 13.7× 9.1× 4.0 m full-scale Texas Tech building showing windward roof edge panels A (1.0× 0.2 m^2) and B (1.0× 1.8 m^2)

internal pressures were measured at a number of taps on the test building during strong winds. The pressure signals were low pass filtered at 8 Hz, and sampled at 40 Hz for 15 mins for a single run. The results obtained were from averaging data collected from upto five separate runs. The standard convention of defining positive and suction pressures as acting towards and away from the surface is used. The net (i.e., external-internal) pressures acting into and away from the inside of the building are defined positive and negative respectively.

Data obtained for wind directions (θ) of 90° ± 5° (i.e., approach flow normal to the 9.1 m wall) with a dominant windward wall window opening area of 0.8 m^2 (i.e., 2% of wall) are presented in this paper. External pressures were measured near the roof windward edge at tap positions 50901 and 50905, defined in Levitan and Mehta (1992). The internal pressure was measured at different points within the building shown in Fig. 3. The pressure characteristics on 1.0 m× 0.2 m area A (pressure on tap 50901) and 1.0 m× 1.8 m area B (averaged pressure on taps 50901 and 50905) representative of a cladding fastener and a batten truss tributaries respectively are studied in detail.

The CSTS model study was carried out in the 2.0 m high× 2.5 m wide× 22 m long Boundary Layer Wind Tunnel at the School of Engineering, at James Cook University. The approach Atmospheric Boundary Layer was simulated at between terrain category 2 and 3 as per AS1170.2 at a length scale of 1/50, as shown by the mean velocity referenced to the mean velocity at 10 m, and turbulence intensity profiles in Fig. 4. The scale of turbulence was about 3 times smaller than the target value, which is an acceptable level of relaxation for these types of wind tunnel studies. A typical, 15.6 (*b*)× 7.5 (*d*) × 2.5 (*h*) m low-rise house with a roof pitch of 20° shown in Fig. 5, was constructed at a length scale of 1/50 and tested in this simulated flow. The roof trusses identified as A, B, C, …. N, were spaced 1.2 m apart. Each roof truss tributary was divided into twelve panels identified as 1, 2, 3, …. 12, representing areas supported by batten-truss connections. Panels 1 and 12 were under the eaves.

Ginger *et al.* (1998), measured the external pressures on these panels for approach wind directions (θ) of 0° to 90° at intervals of 15° using a tubing, Scanivalve and transducer system. The pressures were sampled at 500 Hz for 30 secs (equivalent to about 12 min in full-scale) and statistically analysed to give mean, standard deviation, maximum and minimum values in a single run. The

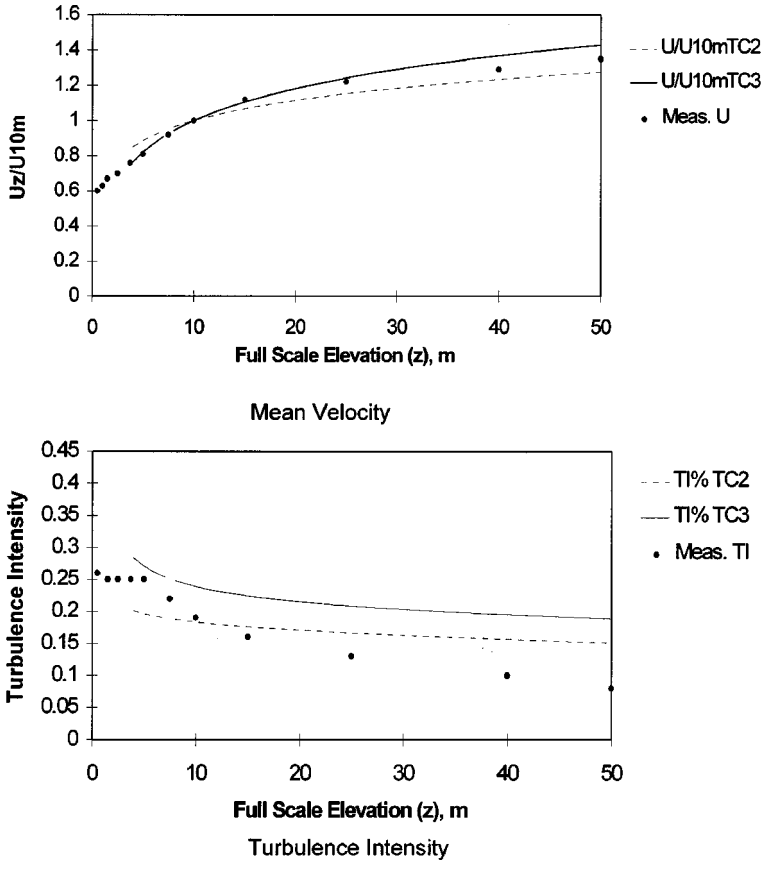

Fig. 4 Atmospheric Boundary Layer simulation at a length scale of 1/50 in the wind tunnel

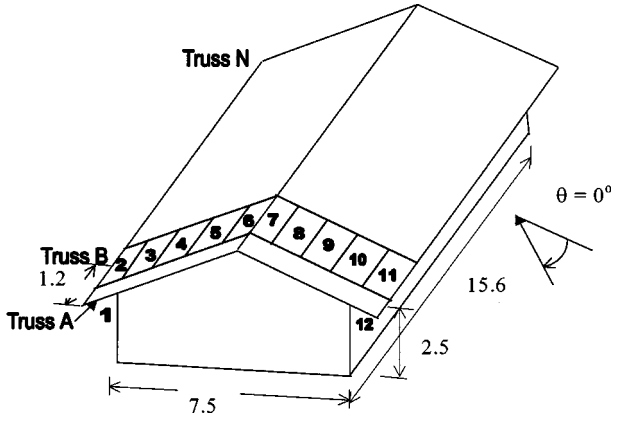

Fig. 5 Typical 15.6× 7.5× 2.5 m, 20° roof pitch CSTS model house tested at 1/50 in the wind tunnel

results obtained from averaging five runs, showed that the panels near the windward gable end and ridge experience large suction pressures. The pressure characteristics within the flow separation

regions near the eaves, ridge and gable end, and the inner part of the roof for a range of approach wind directions, θ were selected for study. Each panel area on the roof is identified by the truss and panel numbers, such that B06 refers to Panel 6 on Truss B.

4 Results

Tables 1 and 2 give the pressure coefficients and pressure peak factors obtained from the Texas Tech full-scale study and the CSTS model study and peak C_ps derived from AS1170.2. In AS1170.2, design peak pressure for cladding elements are determined using a quasi-steady approach, by multiplying a mean pressure coefficient by the design 3 sec gust pressure and the local pressure factor, as described by Eq. (2).

Table 1 Pressure coefficients and pressure peak factors on the Texas Tech full-scale building

Tributary	Area, m^2	$C_{\bar{p}}$	$C_{\hat{p}}$	$C_{\check{p}}$	$C_{\sigma p}$	$g_{\hat{p}}$	$g_{\check{p}}$	K_l	$C_{\hat{p},\check{p}}$
			Measured						AS1170.2*
θ = 90°									**θ = 90°**
Internal		0.65	2.80	-0.24	0.40	5.37	-2.23		2.14
A	0.2 (0.06a^2)	-1.43	-0.28	-7.10	0.60	1.93	-9.52	2.0	-5.51
B	1.8 (0.54a^2)	-1.37	-0.31	-4.50	0.54	1.99	-5.81	1.74	-4.82
A Net	0.2 (0.06a^2)	-2.08	-0.34	-8.36	0.88	1.97	-7.14		-7.65
B Net	1.8 (0.54a^2)	-2.02	-0.35	-6.36	0.84	1.97	-5.14		-6.96

*Velocity gust factor G_U at roof height = 1.75
'a' = minimum of (0.2b, 0.2d, h) = 1.82 m

Table 2 External pressure coefficients and pressure peak factors on the CSTS model house

Tributary	Area, m^2	$C_{\bar{p}}$	$C_{\hat{p}}$	$C_{\check{p}}$	$C_{\sigma p}$	$g_{\hat{p}}$	$g_{\check{p}}$	K_l	$C_{\hat{p},\check{p}}$
			Measured						AS1170.2**
θ = 30°								**θ = 0°**	
A04	0.79 (0.35a^2)	-1.28	-0.20	-3.49	0.42	2.54	-5.23	1.86	-3.92
A06	0.36 (0.16a^2)	-1.68	-0.31	-4.79	0.57	2.43	-5.49	2.0	-4.22
B04	1.57 (0.70a^2)	-0.77	-0.06	-2.44	0.29	2.45	-5.77	1.44	-3.04
B06	0.71 (0.32a^2)	-1.44	-0.30	-4.27	0.50	2.27	-5.65	1.96	-4.13
D06	0.71 (0.32a^2)	-1.03	-0.22	-2.89	0.33	2.38	-5.63	1.90	-4.01
G09	1.57 (0.70a^2)	0.08	0.89	-0.55	0.15	5.24	-4.10	1.0	-1.16, 0.47
θ = 90°								**θ = 90°**	
A04	0.79 (0.35a^2)	-0.76	0.32	-3.27	0.36	3.04	-7.03	1.86	-5.89
A06	0.36 (0.16a^2)	-0.76	0.27	-3.45	0.39	2.64	-6.92	2.0	-6.32
B04	1.57 (0.70a^2)	-0.63	0.42	-2.52	0.31	3.35	-6.07	1.44	-4.55
B06	0.71 (0.32a^2)	-0.60	0.44	-2.78	0.33	3.21	-6.72	1.96	-6.21
D06	0.71 (0.32a^2)	-0.12	0.77	-1.59	0.20	4.35	-7.19	1.90	-6.01
G09	1.57 (0.70a^2)	0.03	0.52	-0.48	0.09	5.16	-5.47	1.0	-1.76

**Velocity gust factor G_U at roof height = 1.875
'a' = minimum of (0.2b, 0.2d, h) = 1.5 m

$$\hat{p}, \breve{p} = \left(\frac{1}{2}\rho \widehat{U}_{3s}^2\right) \times C_p \times K_l \tag{2}$$

The effective AS1170.2 peak design pressure coefficient, $C_{\hat{p},\breve{p}}$ is related to the mean pressure coefficient, C_p and velocity gust factor, $G_U = (\widehat{U}_{3s}/\overline{U})$ as shown in Eq. (3).

$$C_{\hat{p},\breve{p}} = C_p \times K_l \times (\widehat{U}_{3s}/\overline{U})^2 = C_p \times K_l \times G_U^2 \tag{3}$$

The local pressure factor, K_l calculated as per AS1170.2 depends on the extent and location of the tributary area under consideration. The velocity gust factors, G_U at roof height in the Texas Tech full scale building and the CSTS model building are 1.75 and 1.875 respectively. The dimension '*a*' used in calculating the local pressure factor, K_l for the Texas Tech full scale building and the CSTS model building are 1.82 m and 1.5 m respectively.

Internal, external and net C_p vs time plots for $\theta = 90^o$ on areas A and B of the Texas Tech building with a 2% windward wall opening are shown in Figs. 6 and 7 respectively. The probability distributions of pressure fluctuations on areas A and B are compared with the Gaussian form in Figs. 8 and 9 respectively. Figs. 10 and 11 show the probability distributions of external pressure fluctuations on batten-truss tributary panels in edge and inner areas of the CSTS model building roof for $\theta = 30^o$ and 90^o respectively.

Table 1 shows that large external suction and net uplift $C_{\breve{p}}$s were measured on areas A and B of the Texas Tech building. The net uplift $C_{\breve{p}}$ on area A, exceeded values derived from AS1170.2 but compared favourably on area B. External and net pressure peak factors $g_{\breve{p}}$ on areas A and B were less than −7 and −5 respectively, indicating the negative skewness in $p_f(g_p)$ seen in Figs. 8 and 9.

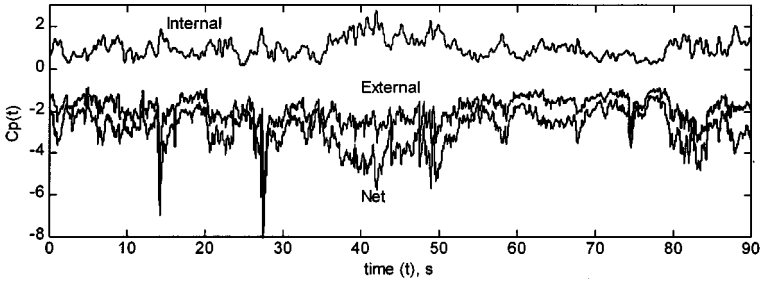

Fig. 6 Part of internal, external and net C_p vs time on area A, Texas Tech full-scale building

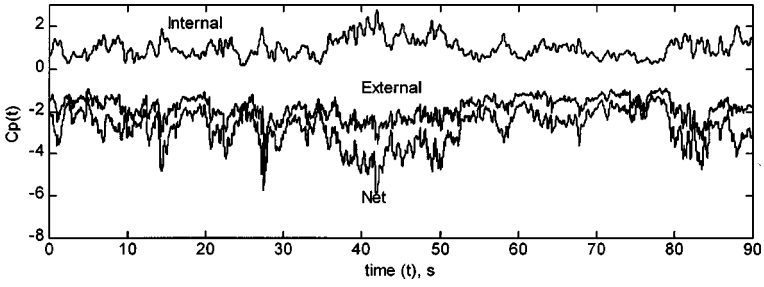

Fig. 7 Part of internal, external and net C_p vs time on area B, Texas Tech full-scale building

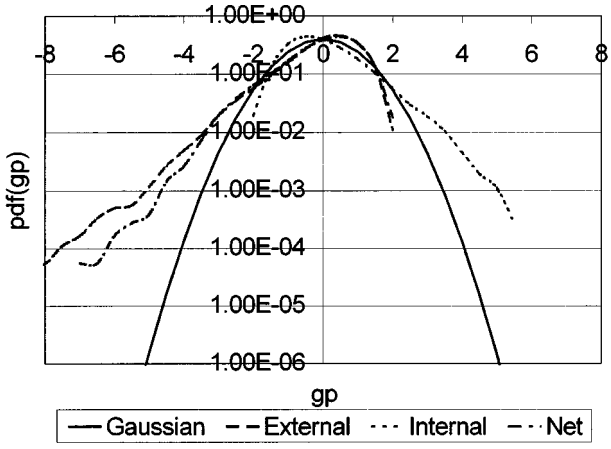

Fig. 8 Probability density functions of internal, external and net pressures on area A, Texas Tech building

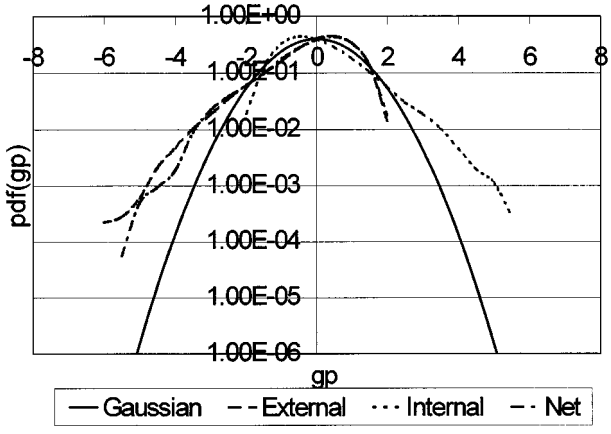

Fig. 9 Probability density functions of internal, external and net pressures on area B, Texas Tech building

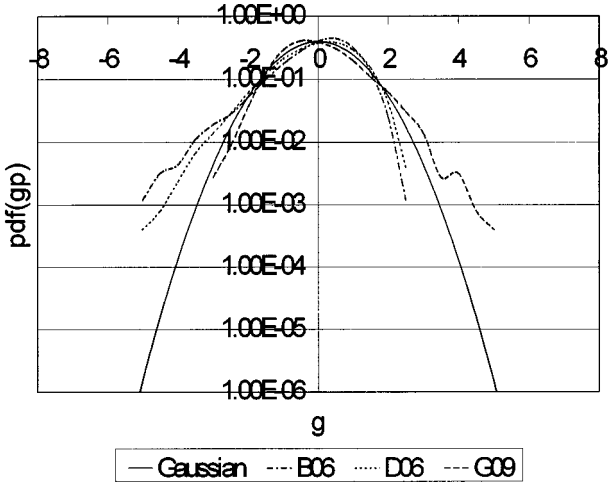

Fig. 10 Probability density functions of external pressures on panels B06, D06 and G09, CSTS model, $\theta = 30^{o}$

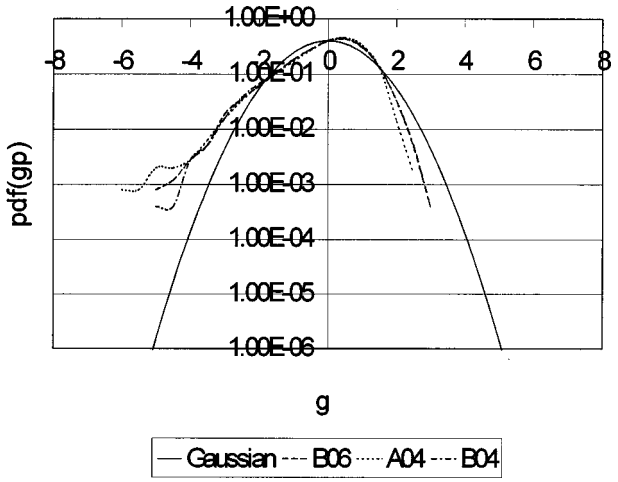

Fig. 11 Probability density functions of external pressures on panels B06, A04 and B04, CSTS model, $\theta = 90^{o}$

The CSTS model test results in Table 2, show that large external suction $C_{\bar{p}}$s were measured on panel areas near the ridge and windward gable end, where pressure peak factors $g_{\bar{p}}$ were less than −5 and $p_f(g_p)$s were negatively skewed. In the inner roof regions (i.e., G09), $g_{\bar{p}}$s were about −4 and $p_f(g_p)$s were closer to Gaussian. Although pressures on a cladding fastener (area 0.2 m^2) can be underestimated, AS1170.2 gives satisfactory net design C_ps on areas of 1.5 to 2.0 m^2 near roof edges.

The external, internal and net pressure spectra, $S_p(f)/(\sigma_p)^2$ on areas A and B of the full-scale Texas Tech building are shown in Figs. 12 and 13. The net pressure spectra are influenced by external and internal pressure fluctuations. The effect of internal pressure Helmholtz resonance

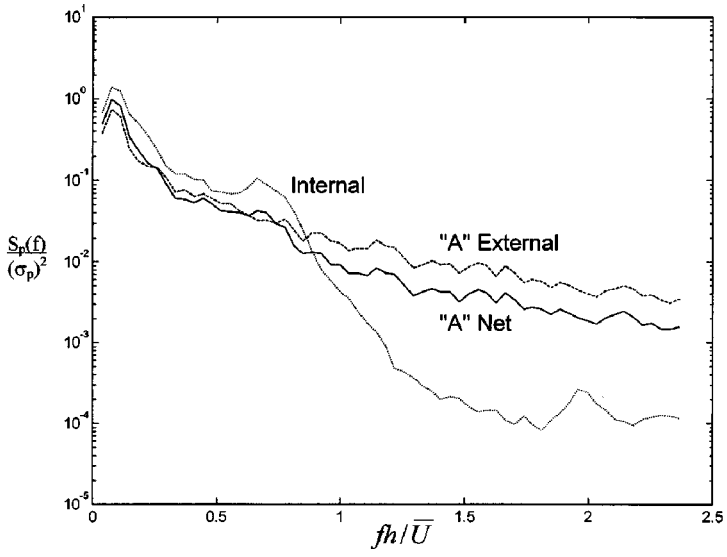

Fig. 12 Internal, external and net pressure spectra on area A, Texas Tech building

described by Ginger and Letchford (1999), is indicated by the increased energy at $fh / \overline{U} \sim 0.6$. The external pressure spectra, $S_p(f) / (\sigma_p)^2$ on the CSTS model building, on areas B06, D06 and G09 for $\theta = 30^o$ and B06, A04 and B04 for $\theta = 90^o$ are shown in Figs. 14 and 15 respectively. The full-scale and model scale spectra have similar characteristics, with the fluctuating pressure energy mostly contained upto $fh / \overline{U} = 0.3$ (i.e., 0.6 Hz in full-scale).

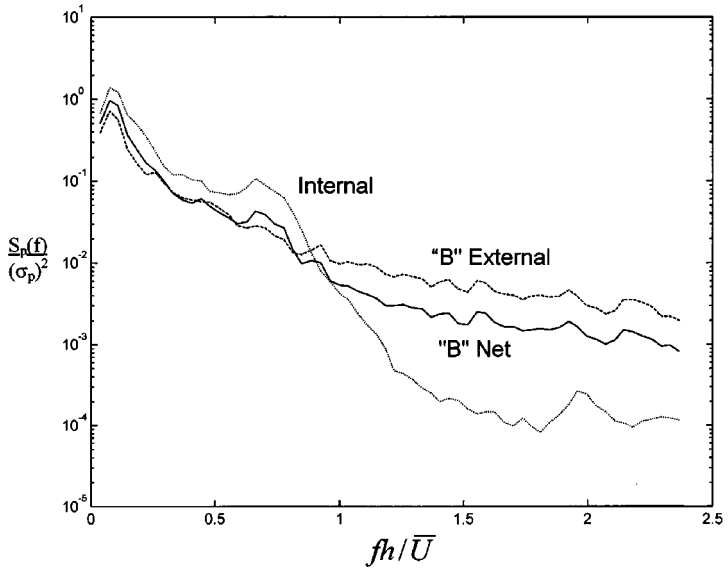

Fig. 13 Internal, external and net pressure spectra on area B, Texas Tech building

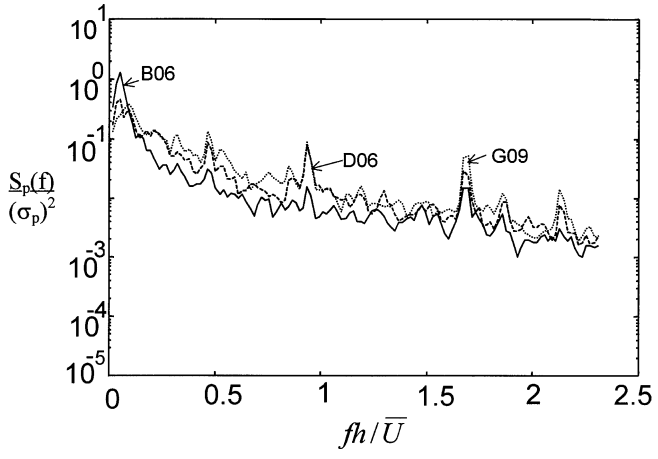

Fig. 14 External pressure spectra on panels B06, D06 and G09, CSTS model house, $\theta = 30^o$

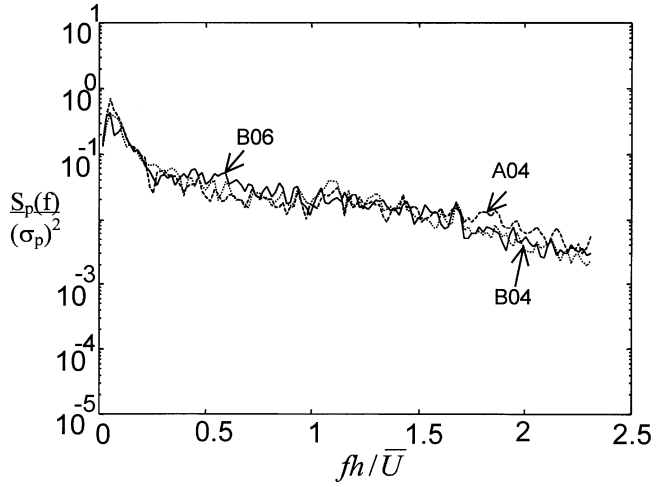

Fig. 15 External pressure spectra on panels B06, A04 and B04 CSTS model house, $\theta = 90^o$

5. Conclusions

The following conclusions are made from analysing pressure measurements on the roofs of the full-scale Texas Tech building and a model of a typical house.

- Large external suction and net uplift pressures were experienced on roof areas of $0.07a^2$ (i.e., cladding fastener tributary) to $0.7a^2$ (i.e., batten-truss connection tributary) within a distance of $0.5a$ and $1.0a$ respectively from the windward edge and ridge.
- AS1170.2 prescribes satisfactory design pressure coefficients C_p and local pressure factors K_l, on batten-truss connection tributary areas, but can underestimate peak design pressures on cladding fasteners near the windward edges.
- The characteristics of pressure fluctuations on batten-truss and cladding fasteners are similar.
- The probability density function of pressure fluctuations on these areas are negatively skewed from the Gaussian form, with pressure peak factors generally less than –5.5.
- The pressure spectra indicate that most of the pressure energy in these areas is contained up to full-scale frequencies of ~ 0.6 Hz

Acknowledgements

The author wishes to thank the Director, Wind Engineering Research Center at Texas Tech University, Dr. Kishor Mehta and his staff for providing the opportunity to collect and use the full-scale data used in this study.

References

Australian Standard (1989), SAA Loading Code Part 2 Wind Loads AS1170.2 1989.

Ginger, J.D. and Letchford, C.W. (1993), "Characteristics of large pressures in regions of flow separation", *Jour. Wind Engineering and Industrial Aerodynamics*, **49**, 301-310.

Ginger, J.D. and Letchford, C.W. (1999), "Net pressures on a low-rise full scale building", *Jour. Wind*

Engineering and Industrial Aerodynamics, **83**, 239-250.
Ginger, J.D., Reardon, G.F. and Whitbread, B.J. (1998), "Wind loads on a typical low-rise house", Cyclone Structural Testing Station, James Cook University Technical Report No. 46.
Jancauskas, E.D., Walker, G.R. and Mahendran, M. (1989), "Fatigue characteristics of wind loads on roof cladding", *Proc. 2nd Asia Pacific Symposium on Wind Engineering*, Beijing, China.
Levitan, M.L. and Mehta, K.C. (1992), "Texas tech field experiments for wind loads Part I: Building and pressure measurement system, Part II: Meteorological instrumentation and terrain parameters", *Jour. Wind Engineering and Industrial Aerodynamics*, **43**, 1565-1588.
Reardon, G.F., Henderson, D.J. and Ginger, J.D. (1999), "A structural assessment of the effects of cyclone Vance on houses in Exmouth WA", Cyclone Structural Testing Station, James Cook University, Technical Report No. 48.
Technical Record 440 (1983), "Guidelines for the testing and evaluation of products for cyclone-prone areas (TR 440)", Experimental Building Station, Department of Hosing and Construction.
Walker, G.R. (1975), "Report on cyclone Tracy - effect on buildings - December 1974", *Department of Housing and Construction.* **1**.
Xu, Y.L. (1993), "Wind induced fatigue loading on roof cladding of low-rise buildings", Cyclone Structural Testing Station, James Cook University, Technical Report No. 41.